Journal of Physiology (1991), **443**, *pp.* 683–701
With 8 figures
Printed in Great Britain

VOLTAGE-DEPENDENT BLOCK BY MAGNESIUM OF NEURONAL NICOTINIC ACETYLCHOLINE RECEPTOR CHANNELS IN RAT PHAEOCHROMOCYTOMA CELLS

BY C. K. IFUNE* AND J. H. STEINBACH

*From the Department of Anesthesiology and *Neural Sciences Program, Division of Biomedical Sciences, Washington University School of Medicine, 660 South Euclid Avenue, Saint Louis, MO 63110, USA*

(*Received 5 February 1991*)

SUMMARY

1. The effects of Mg^{2+} on the single-channel conductance of neuronal nicotinic acetylcholine receptors were examined using receptors expressed by the rat phaeochromocytoma cell line, PC12. PC12 cells express at least three conductance classes of channels that are activated by acetylcholine, the largest conductance class being the most prevalent. This receptor channel is blocked by intracellular and extracellular Mg^{2+}.

2. The effects of Mg^{2+} are asymmetrical; at a given concentration, internal Mg^{2+} is more effective at blocking outward currents than external Mg^{2+} is at blocking inward currents. Receptor channels are blocked at concentrations of Mg^{2+} that are low compared to the concentration of the main permeant cation, Na^+, and the block is voltage dependent.

3. The block by Mg^{2+} is not complete as Mg^{2+} can permeate the channel. With 80 mM-extracellular Mg^{2+} (no extracellular Na^+), the channel has an inward slope conductance of 2·9 pS.

4. The block by extracellular Mg^{2+} can be described by a one site, two barrier model for the channel which includes a negative surface charge on the external surface of the membrane. The parameters of the model place the binding site for Mg^{2+} at 52% of the membrane field from the outside with an apparent dissociation constant of 14 mM. However, the same parameters cannot describe the block by intracellular Mg^{2+}. The deviations from the model suggest that the receptor channel may have more than one binding site for Mg^{2+}.

INTRODUCTION

Inward rectification is a characteristic feature of macroscopic acetylcholine (ACh)-elicited currents of all mammalian peripheral ganglion cells examined to date (Derkach, Selyanko & Skok, 1983; Hirano, Kidokoro & Ohmori, 1987; Mathie, Cull-Candy & Colquhoun, 1987; Yawo, 1989; Fieber and Adams, 1991), adrenal chromaffin cells (Hirano *et al.* 1987; Maconochie, 1990), and some central nervous

system cells (Mulle & Changeux, 1990; Zhang & Feltz, 1990). We have been studying the rectification of the whole-cell and single-channel currents in the rat phaeochromocytoma cell line PC12 which expresses ganglionic-type nicotinic ACh receptors (Ifune & Steinbach, 1990*b*). While the mechanisms underlying the rectification of whole-cell currents have not been fully elucidated, two voltage-dependent processes have been shown to play a role in determining the extent of the rectification. One is the voltage dependence of channel gating and the other is the rectification of the single-channel current (Yawo, 1989; Ifune & Steinbach, 1990*b*; Mathie, Colquhoun & Cull-Candy, 1990).

In this paper, we focus on the rectification of the single-channel currents. Previously, we determined that the rectification was due to block of the outward single-channel current by internal Mg^{2+} ions (Ifune & Steinbach, 1990*b*). Here, we extend this finding in two ways: first, by examination of the concentration and voltage dependence of the channel block by intracellular as well as extracellular Mg^{2+} and second, by evaluation of whether a one site, two barrier Eyring rate theory model for the Mg^{2+} permeation pathway can describe the block of current flow.

Magnesium ions are known to affect the flow of current through a variety of cation channels including nicotinic ACh receptor channels. Mg^{2+} reduces the conductance of muscle (Adams, Dwyer & Hille, 1980; Magleby & Weinstock, 1980; Dani & Eisenman, 1987), *Torpedo* (Imoto, Mathfessel, Sakmann, Mishina, Mori, Konno, Fukuda, Kurasaki, Bujo, Fujita & Numa, 1986; Imoto, Busch, Sakmann, Mishina, Konno, Nakai, Bujo, Mori, Fukuda & Numa, 1988) and ganglionic ACh receptor channels (Mathie *et al.* 1990; Neuhaus & Cachelin, 1990). For muscle receptors, Dani & Eisenman (1987) have determined that Mg^{2+} has a relatively high affinity for the channel and that it is a permeant cation. Their one site, two barrier model of the muscle nicotinic receptor suggests that block of monovalent current by Mg^{2+} would show the following asymmetry: extracellular Mg^{2+} would block inward currents more effectively than intracellular Mg^{2+} would block outward-going currents.

The sensitivity of nicotinic receptors to Mg^{2+} has been useful in the investigation of the relationship between receptor structure and function. Examining the effects of Mg^{2+} on the single-channel conductance of *Torpedo* ACh receptors, Imoto and his colleagues (1988) have identified amino acid residues that are involved in the permeation of ions through the channel. These specific residues bracket the second membrane spanning region which has been proposed to form the lining of the channel pore (Giraudat, Dennis, Heidmann, Chang & Changeux, 1986; Hucho, Oberthur & Lottspeich, 1986; Imoto *et al.* 1986; Leonard, Labarca, Charnet, Davidson & Lester, 1988) and can influence the sensitivity of the channel to block by Mg^{2+} as well as the sidedness of the block (Imoto *et al.* 1988).

In this paper, we demonstrate that the inhibition of single-channel currents through PC12 ACh receptor channels by Mg^{2+} results in a reduced single-channel conductance, the effect being similar to that of Mg^{2+} on the muscle and *Torpedo* nicotinic receptors. The effects of Mg^{2+} are asymmetrical, but in contrast to muscle receptors, intracellular Mg^{2+} is more effective at blocking outward currents than extracellular Mg^{2+} is at blocking inward currents. Mg^{2+} appears to have a relatively high affinity for the PC12 receptor channel and Mg^{2+} does permeate the channel. These observations parallel those reported by Neuhaus & Cachelin (1990). However,

contrary to what was reported by Neuhaus & Cachelin (1990), we show that the Mg^{2+} block is voltage dependent and that a one site, two barrier model for the channel can qualitatively describe most of the features of the block.

METHODS

Cell culture

The PC12H cell line (Hatanaka, 1981) was generously provided by D. Schubert (Salk Institute, San Diego, CA, USA). Cells were maintained and plated for physiological experiments as described previously (Ifune & Steinbach, 1990*a*). Briefly, cells were grown at 37 °C in Dulbecco's modified Eagles' medium containing 10% heat-inactivated fetal bovine serum and 5% heat-inactivated horse serum (Hazelton Research Products, Lenexa, KS, USA; Irvine, Santa Ana, CA, USA) and were passaged weekly. For electrophysiological experiments, cells were plated onto collagen-coated 35 mm plastic tissue culture dishes (Vitrogen 100, Collagen Corp., Palo Alto, CA, USA), and treated with 4 nM- (100 ng/ml) mouse β-nerve growth factor (kindly provided by E. Johnson, Washington University School of Medicine, St Louis, MO, USA). Cultures were fed three times a week and used 5–10 days after plating.

Physiological recordings

Single-channel records were obtained from outside-out patches using a List EPC-7 patch clamp amplifier (List-Electronic, Eberstadt, Germany). Experiments were performed at room temperature (23–24 °C). Patch pipettes were pulled with a P-80/PC Flaming–Brown electrode puller (Sutter Instruments Co., San Rafael, CA, USA) from KG33 borosilicate capillaries. The pipettes were coated with Sylgard 182 (Dow Corning Corp., Midland, MI, USA) and fire-polished. The resistance of the fire-polished pipettes ranged from 3 to 5 MΩ when filled with a low-chloride solution. Agonist-containing solution was perfused onto outside-out patches with a large diameter (50 μm) pipette placed near the patch (50 μm).

Single-channel current–voltage relationships were determined using voltage ramps that started at −80 mV and linearly increased to +80 mV over 24 ms. The voltage ramps were generated by the CLAMPEX program (Axon Instruments, Foster City, CA, USA). An AI2020 event detector (Axon Instruments) was used to initiate a voltage ramp when a single ACh receptor channel opened in response to 10 μM-ACh. Currents were filtered at 2 or 3 kHz (−3 dB frequency) with an 8-pole Bessel filter (902LPF, Frequency Devices, Haverhill, MA, USA) and digitally sampled every 12 μs. Data were analysed using the BINFITS program (kindly provided by Dr C. Lingle, Washington University School of Medicine). Leak current traces consisting of averaged ramp traces taken in the absence of agonist were subtracted from ramp traces taken in the presence of agonist. Single-channel I–V relationships were averages of leak-subtracted traces in which a receptor channel remained open for the entire voltage ramp duration of 24 ms.

For the recordings in the isotonic Mg^{2+} extracellular solution and for the determination of the conductances of the three classes of channel openings, single-channel currents from outside-out patches were recorded at various holding potentials. Data were stored on tape (Racal 4-DS, Southampton, UK) and analysed at a later time. For analysis, data were filtered at 2 kHz (902LPF Bessel filter, Frequency Devices) and digitally sampled using the FETCHEX program (Axon Instruments). The IPROC program (courtesy of Dr C. Lingle) was used to evaluate the single-channel conductances.

Solutions

The compositions of intracellular and extracellular solutions used in the electrophysiological experiments are presented in Table 1. The Mg^{2+} concentrations in the intracellular solutions were calculated using the stability constants for EDTA, EGTA and HEDTA (Martell & Smith, 1974). The actual free Mg^{2+} concentrations were measured using a divalent cation-sensitive electrode (93–32, Orion Research, Boston, MA, USA). A AgCl-saturated KCl single-junction electrode served as the reference (90–01, Orion Research, Boston, MA, USA). The divalent electrode was calibrated using serial dilutions of a 1M-$MgCl_2$ solution. The test solutions used in the measurement of free

Mg^{2+} concentrations in the intracellular solutions contained 24 mM-KCl in the place of the sodium isethionate. The sensitivity of the divalent cation-sensitive electrode to Na^+ required K^+ to be used as a major cation in these test solutions. The activity of Mg^{2+} in the extracellular solutions was assessed using the divalent cation-sensitive electrode. The test solutions contained 100 mM-potassium isethionate (Eastman Kodak Company, Rochester, NY, USA) in place of the sodium

TABLE 1. Composition of intracellular solutions

Intracellular solutions

Calculated free $[Mg^{2+}]$ (μM)	Measured free $[Mg^{2+}]$ (μM)	NaIse (mM)	NaCl (mM)	$MgCl_2$ (mM)	NaOH (mM)	Chelator (mM)	HEPES (mM)	pH
0	0	70	10	0	76	20 EDTA	40	7·3
30	50	125	0	5	33	10 HEDTA	40	7·4
100	100	125	0	7	32	10 HEDTA	40	7·3
300	300	110	9	0·5	32	10 EGTA	20	7·3
1000	900	110	6	2	34	10 EGTA	20	7·4
3000	2600	116	0	5	37	10 EGTA	20	7·4

Extracellular solutions

Calculated free $[Mg^{2+}]$ (mM)	NaIse (mM)	NaCl (mM)	$MgCl_2$ (mM)	NaOH (mM)	Chelator (mM)	HEPES (mM)	pH
0·05	123	0	5	32	10 HEDTA	20	7·3
1	142	8	1	5	0	20	7·3
3	149	4	1	2	0	20	7·3
10	149	0	10	4	0	20	7·3
30	140	0	30	12	0	20	7·3

The pH was titrated to the specified value with NaOH. The final Na^+ concentrations ranged from 150 to 158 mM. Measured free Mg^{2+} concentrations were determined using a divalent cation-sensitive electrode (see Methods). NaIse, sodium isethionate; EDTA, ethylenediaminetetraacetic acid; EGTA, ethyleneglycol-bis(β-aminoethylether); HEDTA, *N*-(2-hydroxyethyl)ethylenedinitro-*N,N'N'*-triacetic acid; HEPES, hydroxyethylpiperazine-*N'*-2-ethanesulphonic acid.

isethionate. Although a value for the activity coefficient of Mg^{2+} in each of the solutions could not be evaluated, the logarithmic relationship between the electrode potential and the Mg^{2+} concentration suggested that between 1 and 30 mM the activity coefficient for Mg^{2+} stayed relatively constant. Tetrodotoxin (0·5–1 μM) was added to all of the extracellular solutions to block voltage-activated Na^+ channels.

The extracellular solution used in the measurement of single-channel Mg^{2+} currents contained (in mM): 75 magnesium acetate, 5 $MgCl_2$, 20 HEPES, 100 mannitol, and was adjusted to pH 7·3 with magnesium hydroxide. The sodium acetate intracellular solution contained (in mM): 145 sodium acetate, 10 NaCl, 20 HEPES and 10 EDTA. The pH was adjusted to 7·3 with 1 M-acetic acid.

Calculation of surface potentials

To calculate surface potentials, the following relationship between the surface charge and the surface potential was used (Grahame, 1947; Muller & Finkelstein, 1974; Hille, Woodhull & Shapiro, 1975; Lewis, 1979):

$$\sigma^2 = 0{\cdot}37\{\Sigma[i]_o \exp(-zF\psi/RT - 1)\},$$

and the sum was taken over all ions present in the solution. σ is the charge per square nanometer, ψ is the surface potential (mV), $[i]_o$ is the bulk activity of ion i in mol/l, and z is the valency of ion i. Mg^{2+} binding to negative surface charges was not considered. The activity coefficient for sodium isethionate was estimated to be 0·8. Taking into account the relationship between $CaCl_2$ activity and concentration in solutions also containing 150 mM-NaCl (Butler, 1968) and comparing the activity coefficients for $MgCl_2$ and $CaCl_2$ (Goldberg & Nuttall, 1978), a value of 0·55 was chosen for

the activity coefficient of $MgCl_2$. The Guggenheim convention was used to estimate the activity of Mg^{2+} ($g^{2+} = (g_{\pm})^2$, where g^{2+} is the activity coefficient for Mg^{2+} and $g_{\pm}$ is the mean activity coefficient for $MgCl_2$; Shatkay, 1968; Butler, 1968). A Boltzmann relationship was used to calculate the surface activity of the cations:

$$[i]_s = [i]_o \exp(-zF\psi/RT),$$

where $[i]_s$ is the surface activity of ion i.

In order to fit the *I–V* curves predicted from the one site, two barrier blocking model to the observed *I–V* curves, the observed *I–V* curves were transferred into the Sigmaplot program (Jandel Scientific, Corte Madera, CA, USA). The program was used to calculate and plot the theoretical *I–V* relationships. Best fits were determined by visual inspection.

All drugs and chemicals were obtained from Sigma Chemical Company (St Louis, MO, USA) unless specified otherwise.

RESULTS

ACh-elicited single-channel currents

Current recordings were made from outside-out patches. Under the conditions used, few channel openings of any type were seen in the absence of ACh (the solutions had no added K^+ or Ca^{2+}, low Cl^- and external tetrodotoxin). During the application of ACh to the external surface, many channel openings were observed. The response to 5 μM-ACh essentially completely desensitized over 40 s and did not fully recover. The channel activity in outside-out patches showed progressive run-down and could not be maintained for more than 5–7 min (see also Ballivet, Nef, Couturier, Rungger, Bader, Bertrand & Cooper, 1988; Zhang & Feltz, 1990).

Three amplitude classes of single-channel openings were seen during the application of 3–5 μM-ACh. The largest and most prevalent class of openings had a slope conductance of approximately 49 pS (Fig. 1). This class was seen in all outside-out patches examined and depending on the patch comprised 80–100% of openings. Most of the remaining openings were from a smaller conductance channel of about 37 pS. The smallest amplitude class of openings ($\sim$ 25 pS) was only seen very occasionally.

As the largest conductance class of channels was the most prevalent and also had the longest burst duration (C. K. Ifune & J. H. Steinbach, unpublished), current through these channels probably accounted for a major portion of the whole-cell current. Accordingly, we determined the *I–V* relationship of this receptor channel and its dependence on Mg^{2+}.

Block by intracellular Mg^{2+}

The dependence of the *I–V* relationship of the 49 pS channel on intracellular Mg^{2+} concentrations was determined using voltage ramps. A voltage ramp, 24 ms in duration, was initiated after a single-channel opening was detected. The mean burst duration of the ACh receptor channels at -80 mV was approximately 40 ms (C. K. Ifune & J. H. Steinbach, unpublished) and roughly 25% of the initiated ramps resulted in a trace in which the channel remained open for the entire ramp duration. Using a slower ramp (100 ms in duration) did not alter the single-channel *I–V* relationships with 0 and 1 mM-intracellular Mg^{2+} (data not shown).

The effects of increasing the intracellular Mg^{2+} concentration from nominally zero to 3 mM on the single-channel *I–V* relationship are shown in Fig. 2. The extracellular

Mg^{2+} concentration was 1 mM for all the *I–V* traces in this figure. The increase in the intracellular Mg^{2+} concentration had no effect on the reversal potential. When the intracellular Mg^{2+} concentration was nominally zero (20 mM-EDTA, no added divalent cations), the single-channel *I–V* relationships displayed slight outward

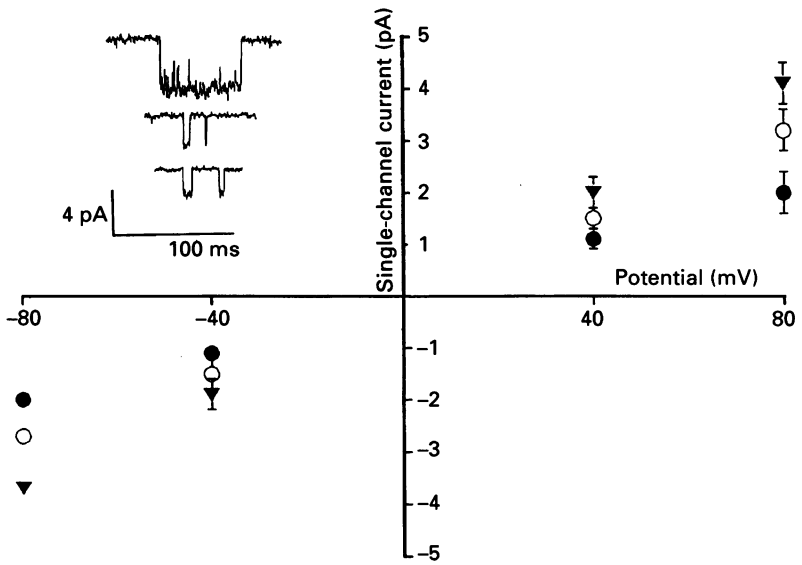

Fig. 1. The symbols represent the mean (±standard deviation) of single-channel amplitudes recorded at steady holding potentials. ●, the *I–V* relationship for the 26 pS channel; ○, the 37 pS channel; ▼, the 49 pS channel. Data at −80 mV were taken from four outside-out patches. Data were gathered from two patches at each of the other potentials. Inset, single-channel openings at −80 mV representative (from top to bottom) of the 49, 37 and 26 pS channels. The intracellular Mg^{2+} concentration was 0 and the extracellular Mg^{2+} concentration was 1 mM.

rectification and the single-channel slope conductance at negative potentials was approximately 50 pS. Increasing the intracellular Mg^{2+} concentration decreased the outward current through the channel. Focusing on the *I–V* relationships with the three highest intracellular Mg^{2+} concentrations, the block of the current appeared to reach a maximum between +20 and +30 mV. Positive to +40 mV, *I–V* relationships curved upward and the single-channel conductance increased. A slight reduction in the magnitude of the inward current was also seen with the increase in intracellular Mg^{2+} concentration. The reduction in current could be described by a single blocking isotherm with a voltage-dependent apparent IC_{50} (concentration giving 50% of maximal inhibition) (Fig. 3).

Block by extracellular Mg^{2+}

The single-channel *I–V* relationship was also sensitive to concentrations of extracellular free Mg^{2+}. Single-channel *I–V* relationships with 0·05, 1, 3, 10 and 30 mM-extracellular Mg^{2+} are shown in Fig. 4. The intracellular Mg^{2+} concentration was nominally zero. As the extracellular Mg^{2+} concentration was increased, the

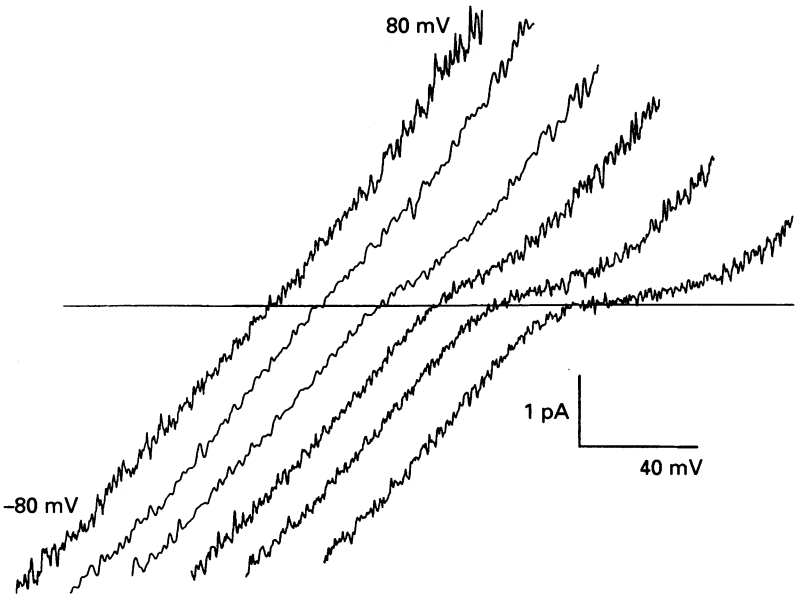

Fig. 2. Single-channel *I–V* relationships with different concentrations of intracellular Mg^{2+}. From left to right, the free intracellular Mg^{2+} concentrations were 0, 0·05, 0·1, 0·3, 0·9 and 2·6 mM. The extracellular Mg^{2+} concentration was 1 mM. All currents reversed close to 0 mV. The current traces have been offset along the abscissa to improve the clarity of the figure. The applied voltage ramp increased linearly from −80 (left) to +80 (right) mV in 24 ms. Each trace is the average of thirteen to twenty leak-subtracted current traces. All traces were low-pass filtered at 3 kHz except for the second and third traces from the left which were filtered at 2 kHz.

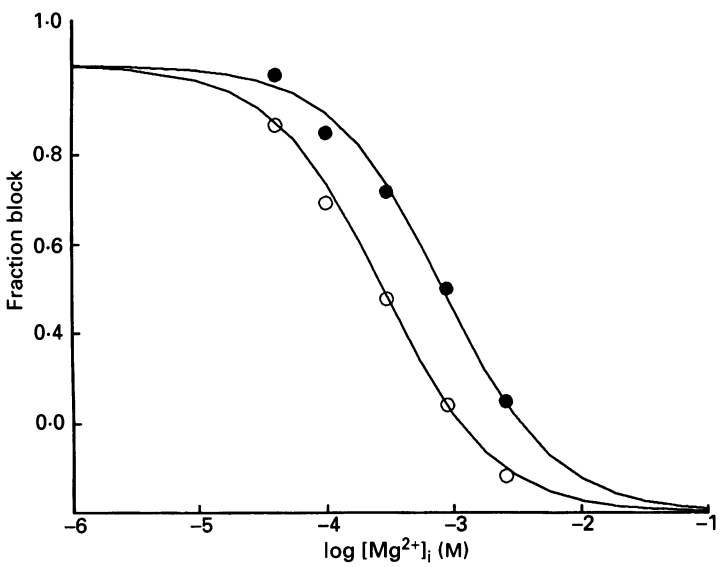

Fig. 3. Normalized single-channel currents at +30 mV (○) and +80 mV (●) as a function of log $[Mg^{2+}]_i$. Data were taken from the *I–V* curves shown in Fig. 2. The continuous lines were calculated using a single site binding isotherm with an IC_{50} of 280 μM for the +30 mV curve and 830 μM for the +80 mV curve. Note that the fit is reasonably good at both potentials.

inward current through the channel decreased. In addition, extracellular Mg^{2+} reduced outward current through the channel. A shift in the reversal potential was not seen as the extracellular Mg^{2+} concentration was increased; all the current traces reversed at or close to 0 mV. When the extracellular Mg^{2+} concentration was 50 μM

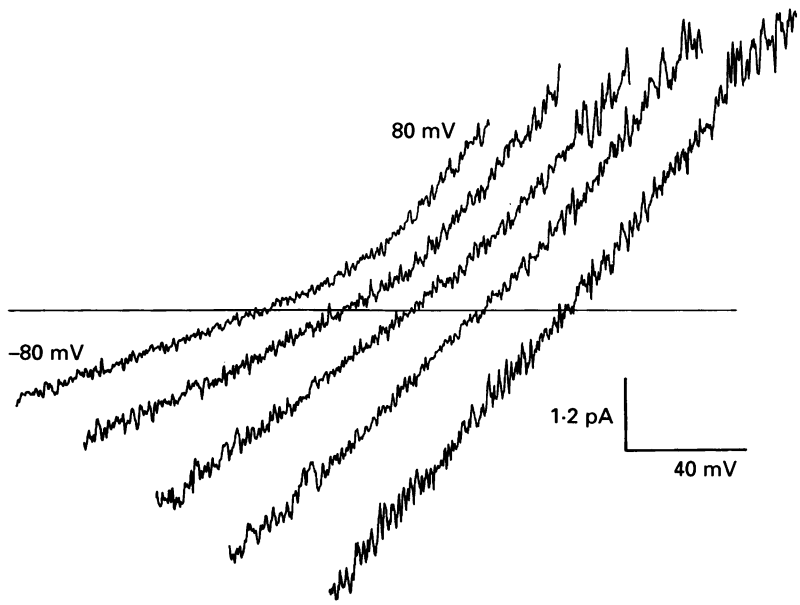

Fig. 4. Single-channel *I–V* relationships with different concentrations of extracellular Mg^{2+}. From right to left, the free extracellular Mg^{2+} concentrations were 0·05, 1, 3, 10 and 30 mM. The intracellular Mg^{2+} concentration was nominally zero. The reversal potential for all the traces was 0 mV. The current traces have been offset along the abscissa for clarity. The *I–V* relationships were determined using voltage ramps (see Fig. 2). Traces were low-pass filtered at 3 kHz.

and the intracellular Mg^{2+} concentration was 0, the single-channel *I–V* relation was linear and the slope conductance was 60 pS (the presence of some extracellular Mg^{2+} was needed to prevent the development of a large non-specific leak current).

The fractional block at −80 mV as a function of extracellular Mg^{2+} concentration could not be well described by a simple blocking isotherm. The curve is shallower than that expected for channel block by a single Mg^{2+} ion (Fig. 5; ○). Later it will be shown that the apparent deviation from one-to-one binding can be explained by the effects of a surface charge on the external face of the membrane (Fig. 5; ●).

Single-channel currents carried by Mg^{2+}

As shown above, Mg^{2+} blocks PC12 ACh receptor channels, but it is a permeant cation as well. Small single-channel openings in response to ACh can be seen with an isotonic magnesium acetate extracellular solution (inset to Fig. 6). The *I–V* relationship with 155 mM-intracellular sodium and 80 mM-extracellular magnesium is shown in Fig. 6. The reversal potential for the current was approximately +30 mV, and the inward Mg^{2+} current has a slope conductance of 2·9 pS.

A model for the block by Mg^{2+}

The results presented so far demonstrate that Mg^{2+} ions produce voltage-dependent block of Na^+ currents through these nicotinic ACh receptor channels, that block can be produced by either intracellular or extracellular Mg^{2+}, and that Mg^{2+}

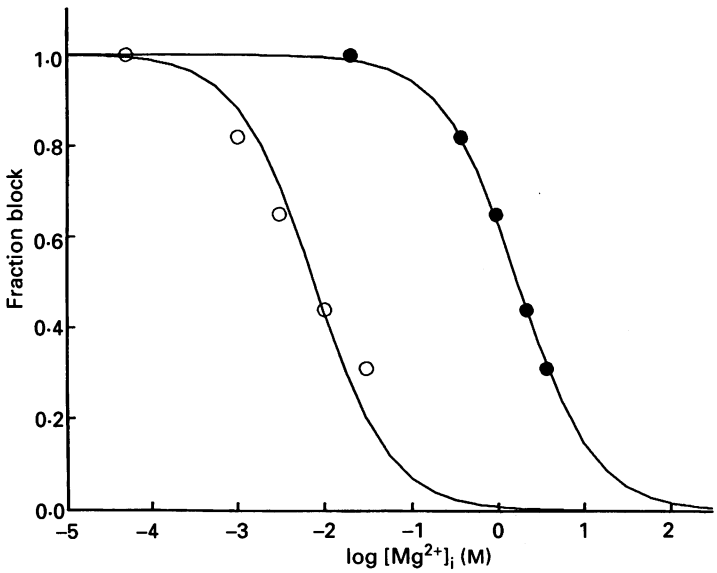

Fig. 5. Normalized single-channel currents at −80 mV as a function of log $[Mg^{2+}]_o$. ○, uncorrected data taken from the *I–V* curves shown in Fig. 4. ●, normalized single-channel currents at −80 mV as a function of the logarithm of the corrected extracellular Mg^{2+} concentration. The adjustment was made by taking into account the effects of a negative surface charge of $5{\cdot}6 \times 10^{13}$ e cm^{-2} on the extracellular face of the membrane. The concentrations were calculated using a Boltzmann relationship (see Methods). The continuous lines were calculated using a single site binding isotherm with IC_{50} of 7·5 mM (without surface charge) and 1·69 M (with surface charge). Note that the fit to the uncorrected data is less adequate than to the data with corrected concentrations.

can permeate the channel. A simple two barrier, one site model, based on the scheme developed by Woodhull (1973), was used to describe the block by Mg^{2+}. In the most general form, Mg^{2+} ions can get to the binding site in the channel from either the cytoplasmic or the extracellular side giving rise to the following scheme:

$$[Mg^{2+}]_o \underset{k_{-1}}{\overset{k_1}{\rightleftharpoons}} Mg^{2+}\text{–site} \underset{k_{-2}}{\overset{k_2}{\rightleftharpoons}} [Mg^{2+}]_i,$$

where k_1, k_{-1}, k_2 and k_{-2} are voltage-dependent rate constants and $[Mg^{2+}]_i$ and $[Mg^{2+}]_o$ are the free intracellular and extracellular Mg^{2+} concentrations, respectively. In applying this model, the following assumptions were made. (1) The binding and unbinding of the Mg^{2+} ion is assumed to be exponentially dependent on voltage such that $k(E) = k(0)\exp(-zdE/RT)$, where $k(0)$ is the value for the rate constant at zero potential, d is a fraction of the membrane field, E is the potential across the membrane, and R and T have their usual meanings. (2) The binding of Mg^{2+} to the

site is not affected by other ions. (3) When Mg^{2+} is bound to the site within the channel, no ions can pass through the channel and the current carried by Mg^{2+} is assumed to be negligible. (4) Finally, the model requires that the block is at steady state at each point during the voltage ramp. There is evidence to suggest that this

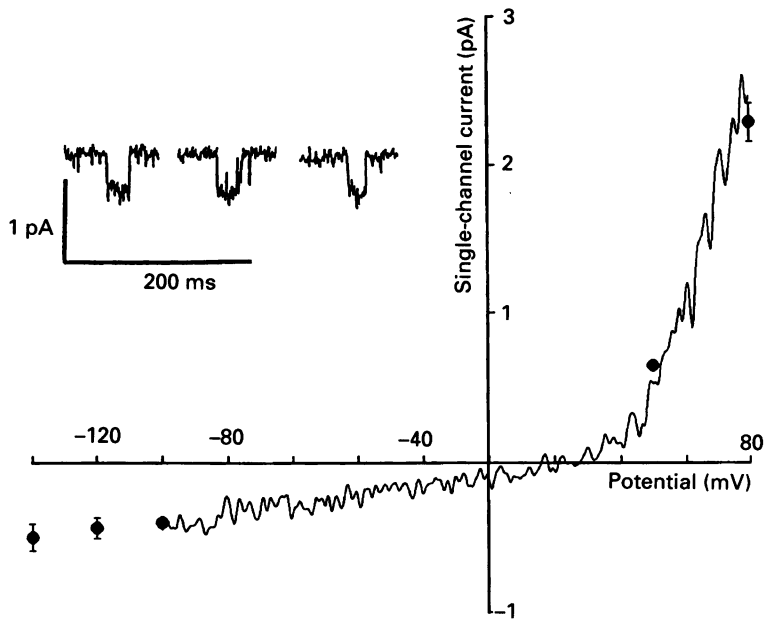

Fig. 6. Single-channel currents carried by Mg^{2+}. The cation in the extracellular solution was 80 mM-Mg^{2+} and the intracellular cation was 155 mM-Na^+. The *I–V* relationship was determined using voltage ramps that started at −100 mV and increased to +80 mV in 24 ms. The current trace is an average of six leak-subtracted traces filtered at 2 kHz. ●, mean (±standard deviation) single-channel current amplitudes recorded at steady holding potentials (n = 5–30 channel openings). The inset shows sample inward currents carried by Mg^{2+} at a holding potential of −120 mV. The current reversed at +30 mV and the inward slope conductance was 2·9 pS.

assumption is correct. Following voltage jumps during single-channel openings, the single-channel currents do not display any relaxation in the presence of Mg^{2+} (Ifune & Steinbach, 1990*b*). This would imply that the block is instantaneous on the time scale of these experiments.

In terms of this scheme, characteristics of the data such as the asymmetrical effects of intracellular and extracellular Mg^{2+} and the concentration dependence of the block would suggest that the energy barriers for Mg^{2+} are asymmetrical, the outer barrier being higher than the inner barrier. The lack of complete block of currents by Mg^{2+} can be explained if Mg^{2+} can permeate the channel. Finally, Mg^{2+} would be expected to have a higher affinity for the binding site than Na^+.

The probability that a channel is not blocked by Mg^{2+} as a function of potential (E) and magnesium concentration ($[Mg^{2+}]$) is given by the following expression:

$$p(E, Mg^{2+}) = (k_{-1}+k_2)/(k_1[Mg^{2+}]_o + k_{-1} + k_2 + k_{-2}[Mg^{2+}]_i). \quad (1)$$

For block by Mg^{2+} from the extracellular side (note that the concentration of intracellular Mg^{2+}, $[Mg^{2+}]_i$, is 0), the expression for the current as a function of voltage and Mg^{2+} concentration is given by:

$$i(E,[Mg^{2+}]_o) = i(E,0)\,(1+G_o(E))/(1+G_o(E)+F_o(E)[Mg^{2+}]_o), \quad (2)$$

where $G_o(E) = k_2(E)/k_{-1}(E)$ and $F_o(E) = k_1(E)/k_{-1}(E)$. The term $i(E,0)$ is the single-channel current in the absence of intracellular and extracellular Mg^{2+}. However, as it was not possible to remove Mg^{2+} from both sides and keep the outside-out patch intact, the *I–V* relationship with 0 intracellular Mg^{2+} and 50 μM-extracellular Mg^{2+} was used for $i(E,0)$. In Fig. 7*A*, the dotted lines were obtained by adjusting parameters $G_o(E)$ and $F_o(E)$ until the lines fitted the data points. Here, $G_o(E) = 4{\cdot}5\exp(-E\times 0{\cdot}042\ \mathrm{mV^{-1}})$ and $F_o(E) = 870\ \mathrm{M^{-1}}\exp(-E\times 0{\cdot}042\ \mathrm{mV^{-1}})$. These parameters can describe the *I–V* relationships with 0·05 and 1 mM-extracellular Mg^{2+}, but as the extracellular Mg^{2+} concentration is increased, the calculated *I–V* relationships deviate from the observed ones. At the two highest concentrations of extracellular Mg^{2+} (10 and 30 mM), the discrepancy is quite large; more block is predicted than is observed for both inward and outward currents. The poor agreement between the theoretical and observed curves is not dependent on voltage, but on concentration. The deviation increases as the Mg^{2+} concentration is increased. A possible explanation is the presence of a surface potential at the extracellular face of the membrane which would enhance the effective concentration at the mouth of the channel at low extracellular Mg^{2+} concentrations, but not at high concentrations.

The effects of a uniformly distributed negative extracellular surface charge were incorporated into the blocking model. The surface potential as a function of surface charge and ionic concentration was calculated using the Gouy-Chapman relationship (Grahame, 1947; Muller & Finkelstein, 1974; Hille *et al.* 1975; Lewis, 1979) and a Boltzmann relationship was used to estimate the surface activity of Mg^{2+} (see Methods for the calculation of the surface potential). The relationship between the single-channel current, the membrane potential and $[Mg^{2+}]_o$ in the presence of a surface potential, ψ, is given by the following expression:

$$i(E,[Mg^{2+}]_o) = I(E,0)\,(1+G_o(E-\psi))/(1+G_o(E-\psi)+F_o(E-\psi)\,[Mg^{2+}]_o\exp(-zF\psi/RT)). \quad (3)$$

The value of the surface charge determined the regularity of the spacing between the *I–V* curves with different external Mg^{2+} concentrations. A surface charge of $5{\cdot}6\times 10^{13}$ e $\mathrm{cm^{-2}}$ was chosen as it enabled all the curves to be fitted simultaneously. With the addition of a negative surface potential to the model, the agreement between the calculated and observed *I–V* relationship was quite good (Fig. 7*b*). The parameters used in the fitting were $G_o(E) = 120\exp(-E\times 0{\cdot}042\ \mathrm{mV^{-1}})$ and $F_o(E) = 70\ \mathrm{M^{-1}}\exp(-E\times 0{\cdot}042\ \mathrm{mV^{-1}})$. From the voltage dependence of $F_o(E)$, the binding site for Mg^{2+} is calculated to be 52% of the membrane field from the outside. The apparent dissociation constant at zero potential is about 14 mM.

The presence of an external surface charge also provides an explanation for the deviation of the fractional block as a function of extracellular Mg^{2+} concentration from a single site blocking isotherm (Fig. 5; ●). The addition of the surface charge

alters the curve in two ways. First, it increases the apparent dissociation constant because the surface charge increases the effective Mg^{2+} concentration. Second, since the surface charge is more effective at increasing the local Mg^{2+} concentration of lower Mg^{2+} concentrations than higher ones, the relationship between fractional

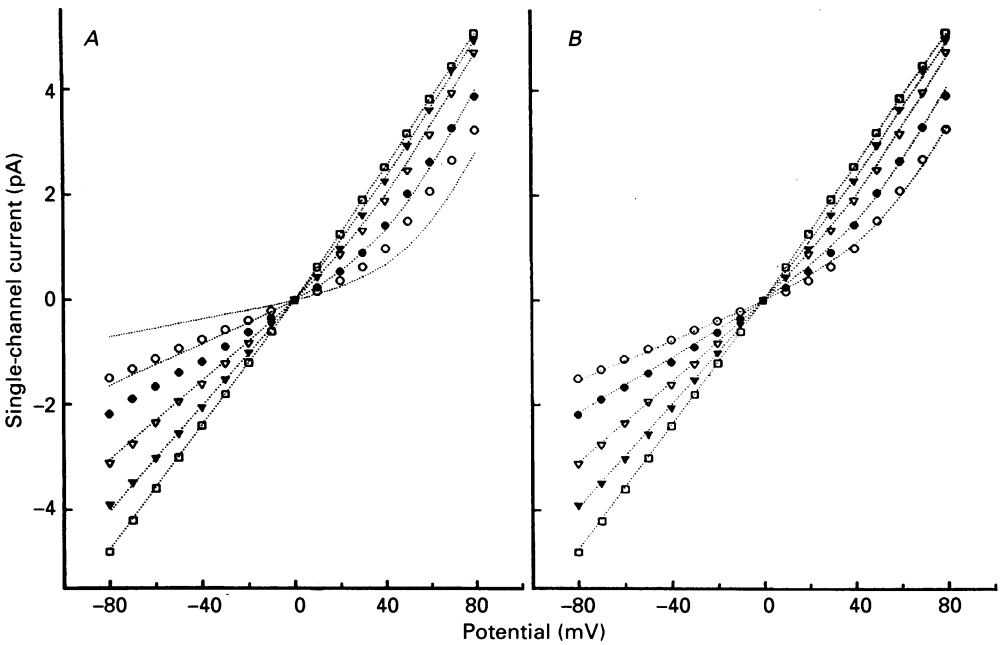

Fig. 7. The one site, two barrier model fitted to the observed *I–V* relationships with different extracellular Mg^{2+} concentrations. These *I–V* relationships with 50 μM (□), 1 mM (▼), 3 mM (▽), 10 mM (●) and 30 mM (○) extracellular Mg^{2+} are identical to those presented in Fig. 4. Panel *A* shows the theoretical curves calculated using eqn (2) (dotted lines). The parameters used were $F_o(E) = 870\ M^{-1} \exp(-E \times 0{\cdot}042\ mV^{-1})$ and $G_o(E) = 4{\cdot}5 \exp(-E \times 0{\cdot}042\ mV^{-1})$. Note that the fit is satisfactory for lower concentrations of Mg^{2+}, but poor for both inward and outward currents with 10 mM- and 30 mM-external Mg^{2+}. Panel *B* shows that including a negative surface charge (eqn (3)) results in an adequate fit for all Mg^{2+} concentrations. Parameters used were $F_o(E) = 70\ M^{-1} \exp(-E \times 0{\cdot}042\ mV^{-1})$ and $G_o(E) = 120 \exp(-E \times 0{\cdot}042\ mV^{-1})$. The surface charge was $5{\cdot}6 \times 10^{13}$ e cm^{-2}.

block and effective Mg^{2+} concentration is steeper and is well described by a one-to-one blocking stoichiometry.

According to the one site, two barrier model, a complementary set of parameters should be able to describe the block of the channel current by intracellular free Mg^{2+}. The equation used to describe block by intracellular Mg^{2+} was:

$$i(E, Mg^{2+}) = i(E, 0)\,(1 + G_i(E-\psi))/\{1 + G_i(E-\psi) + F_i(E-\psi)[Mg^{2+}]_i + H_i(E-\psi)[Mg^{2+}]_o \exp(-2\psi/RT)\},$$

where $G_i(E) = k_{-1}(E)/k_2(E)$, $F_i(E) = k_{-2}(E)/k_2(E)$, and $H_i(E) = k_1(E)/k_2(E)$. Again, $i(E, 0)$ was the *I–V* curve with zero intracellular Mg^{2+} and 50 μM-extracellular Mg^{2+}.

The following constraints were taken into consideration in the derivation of the parameters. $G_i(E)$ must be the reciprocal of $G_o(E)$. If Mg^{2+} binds to a single site within the channel, then the sum of the fractions of the membrane field sensed by the Mg^{2+} ion calculated from the inside and the outside must be one. Finally, when the

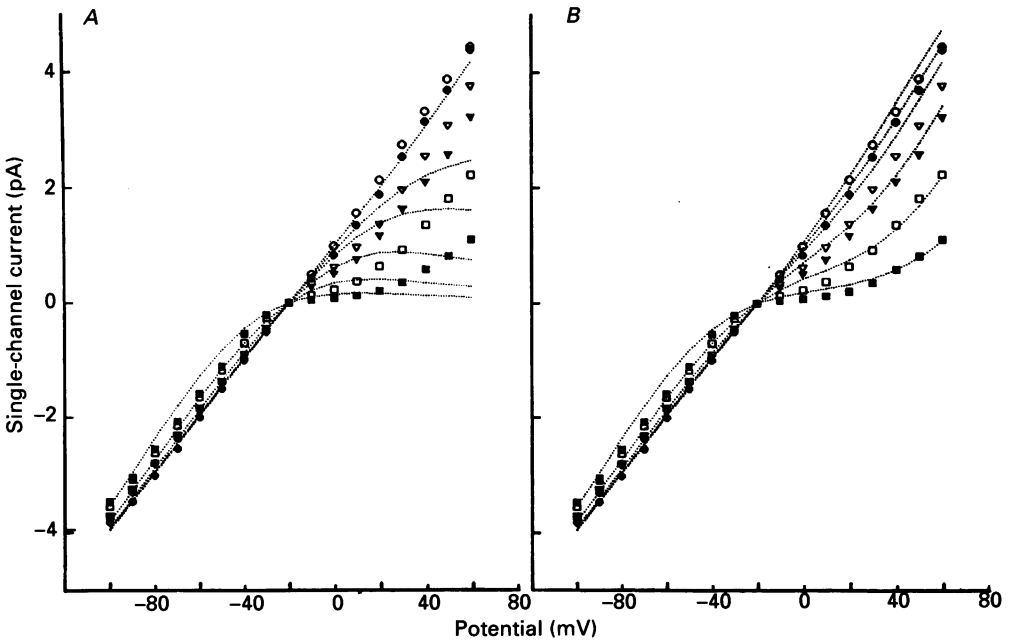

Fig. 8. The one site, two barrier model fitted to the observed *I–V* relationships with different intracellular Mg^{2+} concentrations. These *I–V* relationships with 0 (○), 30 μM (●), 100 μM (▽), 300 μM (▼), 1 mM (□) and 3 mM (■) intracellular Mg^{2+} are the same as those presented in Fig. 2. The theoretical curves (dotted lines) were calculated using eqn (4). Panel *A* shows predicted *I–V* relationships for various internal Mg^{2+} concentrations, assuming values for parameters which were calculated from the values derived from the block produced by extracellular Mg^{2+} (see Fig. 7). The values for the parameters were $G_i(E) = 0{\cdot}0008 \exp(E \times 0{\cdot}042\ \mathrm{mV^{-1}})$, $F_i(E) = 70\ \mathrm{M^{-1}} \exp(E \times 0{\cdot}038\ \mathrm{mV^{-1}})$ and $H_i(E) = 0{\cdot}58$. Panel *B* shows curves predicted when a single parameter (the voltage dependence of the ratio k_2/k_{-1}) was altered. Values for the parameters were $G_i(E) = 0{\cdot}0008 \exp(E \times 0{\cdot}065\ \mathrm{mV^{-1}})$, $F_i(E) = 70\ \mathrm{M^{-1}} \exp(E \times 0{\cdot}038\ \mathrm{mV^{-1}})$ and $H_i(E) = 0{\cdot}58$.

concentration of Mg^{2+} is the same on both sides of the membrane, then at 0 mV there should be no net flow of Mg^{2+}. This requires that $k_{-2}(0)/k_2(0) = k_1(0)/k_{-1}(0)$. The resulting values for the parameters were:

$$G_i(E) = 0{\cdot}008 \exp(E \times 0{\cdot}042\ \mathrm{mV^{-1}}),$$

$$F_i(E) = 70\ \mathrm{M^{-1}} \exp(E \times 0{\cdot}038\ \mathrm{mV^{-1}}),$$

$$H_i(E) = 0{\cdot}58\ \mathrm{M^{-1}}.$$

These parameters do not describe the block by intracellular Mg^{2+} well over the entire voltage range of −80 to +80 mV. The outward currents are poorly described.

At potentials between 0 and about +30 mV, the calculated curves, lying above the observed *I–V* curves, do not predict enough block. Positive to +40 mV, the calculated curves do not curve upward and predict less current than is actually seen. In comparison, the inward currents are better described by the parameters used to model the block by extracellular Mg^{2+} (Fig. 8).

Neither reducing the apparent affinity of the site for Mg^{2+} nor decreasing the voltage dependence of the affinity could introduce any upward curvature into the predicted curves. The single parameter that had a significant effect on the curvature at positive potentials was the voltage dependence of the ratio of the unblocking rates. By increasing the voltage dependence of this ratio from e-fold over 24 mV to e-fold over 15·3 mV, the predicted curves displayed an amount of upward curvature comparable to that seen for the observed *I–V* curves.

Although the agreement between the observed and theoretical *I–V* curves is better when the voltage dependence of the unblocking rates is increased, the fit is not perfect. At positive potentials between +10 and about +30 mV, the calculated curves continue to lie above the *I–V* curves with the three highest intracellular Mg^{2+} concentrations. In addition, for the highest intracellular Mg^{2+} concentration, the inward current is not blocked as strongly as the calculated curve would predict. Other sets of values for $G_i(E)$ and $F_i(E)$ can provide a slightly better fit for the outward-going currents, but they resulted in theoretical *I–V* curves which predicted too much block of the inward currents. Postulating an intracellular surface charge did not increase the quality of the fit, as there were no systematic deviations between the predicted and observed curves that were dependent on Mg^{2+} concentrations. No set of parameters could simultaneously account for the *I–V* curve with 100 μM-intracellular Mg^{2+} and the other curves. The possibility exists that the free Mg^{2+} concentration was underestimated for the 100 μM-intracellular solution.

DISCUSSION

Mg^{2+} ions reduced the current flow through single PC12 ACh receptor channels. Removal of Mg^{2+} from the intracellular and extracellular solutions linearized the single-channel *I–V* relationship and under these conditions, the single-channel conductance with Na^+ as the charge carrier was approximately 60 pS. The reduction of the current had the following qualitative features. Currents were blocked at concentrations of Mg^{2+} that were relatively low compared to the Na^+ concentration. The effects of Mg^{2+} were asymmetrical; intracellular Mg^{2+} was more effective at blocking outward currents than extracellular Mg^{2+} was at blocking inward currents. Also, the block by intracellular Mg^{2+} was described by a single binding isotherm, but block by extracellular Mg^{2+} was not unless the presence of a negative surface charge on the external face of the membrane was postulated. Mg^{2+} can carry current through the channel. The block of current by Mg^{2+} and the relief of block were voltage dependent and qualitatively consistent with a mechanism involving open-channel block and permeation.

To examine the mechanism of the block further, the inhibition of the single-channel current by Mg^{2+} was described with an Eyring rate theory model with one site and two barriers for Mg^{2+} and a negative surface charge on the external face of the membrane. The parameters that provide a good description of the single-channel

current as a function of voltage and extracellular Mg^{2+} concentration suggest that the binding site for Mg^{2+} is located 52% through the membrane field from the extracellular side. ACh receptor channels of rat sympathetic ganglion cells are also blocked by Mg^{2+}. Using a one site, two barrier model to describe the block by intracellular Mg^{2+}, Mathie and his colleagues (1990) estimate that the binding site sees 24% of the membrane field. For muscle-type receptors, Dani & Eisenman (1987) place the binding site 62% through the membrane field. The apparent dissociation constant is 14 mM when the total potential across the membrane is zero. The value for the ratio of the unblocking rates at zero potential indicates that the outer energy barrier for Mg^{2+} is about 5 kT units higher than the inner barrier. The external surface charge density needed to account for the observed concentration dependence of the block of inward current was $5{\cdot}6 \times 10^{13}$ e cm^{-2}. Work by others studying muscle ACh receptors have postulated negative charge densities on outer membrane surfaces ranging from 1·4 to $3{\cdot}3 \times 10^{13}$ e cm^{-2} (Cohen & Van der Kloot, 1978; Lewis, 1979; Adams *et al.* 1980).

However, a single site, two barrier model cannot adequately describe the ability of Mg^{2+} to block currents as a single set of parameters could not provide a quantitative description of both inward and outward currents in the presence of intracellular Mg^{2+}. When using parameters complementary to those used to describe the block by extracellular Mg^{2+} to describe the block by intracellular Mg^{2+}, there was a relatively good description of the inward-going currents. This observation would suggest that once Mg^{2+} is inside the channel, its departure from the channel to the cytoplasmic side can be explained by the proposed one site, two barrier model whether it entered from the extracellular or intracellular side.

In contrast, the one site, two barrier model with the parameters used to describe the block by extracellular Mg^{2+} cannot account for the block of outward currents by intracellular Mg^{2+}. The calculated curves did not predict enough block of the outward currents at potentials between 0 and about +30 mV. A more obvious discrepancy was seen at potentials positive to +40 mV where the degree of unblock was much less than that actually seen. A somewhat better fit to the observed *I–V* curves was achieved by altering a single parameter used to describe the block by intracellular Mg^{2+}. Increasing the voltage dependence of the ratio of the dissociation rates from e-fold over 24 mV to e-fold over 15·3 mV resulted in the upward curvature of the theoretical currents at positive potentials. Although this set of parameters provided a better qualitative description of the observed *I–V* curves, it was still deficient in many ways (Fig. 8*B*). It is quite apparent that at potentials between 0 and +30 mV, the degree of block predicted is less than that observed. In addition, with the highest intracellular Mg^{2+} concentration, the theoretical curve predicted more block of the inward current than was observed.

No set of parameters for the calculated curves could quantitatively account for both the observed degree of block at potentials between 0 and 30 mV and the relief of block at potentials more positive to +40 mV. Although increasing the voltage dependence of affinity of the site for Mg^{2+} increased the level of block at potentials just positive to zero, it also increased the block at the more extreme positive potentials and eliminated the upward swing. The relief of block at potentials positive to +40 mV could be reintroduced by increasing the voltage dependence of the unblocking rates; however, this in turn relieved the block at potentials near zero.

It is likely that a channel with more than one binding site for Mg^{2+} can provide a better description of the block. In some ways, the block of the PC12 nicotinic receptor channels by intracellular Mg^{2+} resembles the block of monovalent cation currents through Ca^{2+} channels by extracellular Ca^{2+}. In both cases, the strongest block occurs at potentials close to 0 mV (Almers & McClesky, 1984). At the more extreme positive and negative potentials, the degree of block is less. Finally, the concentration dependence of the block follows a single site binding isotherm for Ca^{2+} channels (Almers, McClesky & Palade, 1984; Fukushima & Hagiwara, 1985) and PC12 ACh receptor channels (see Figs 3 and 5). The similarities between the block of these two is limited, however. For Ca^{2+} channels, as the Ca^{2+} concentration is raised beyond about 10 μM, the current flow through the channel increases as Ca^{2+} replaces the monovalent cation as the main charge carrier. Such an effect was not seen with PC12 receptor channels as the intracellular Mg^{2+} concentration was increased; there was no evidence for an anomalous mole fraction effect.

The PC12 ACh receptor channel is permeable to Mg^{2+}. This supports the idea that the relief of Mg^{2+} block at positive potentials occurs as Mg^{2+} is pushed through the channel. With 80 mM-extracellular Mg^{2+} and 155 mM-intracellular Na^+, the reversal potential for the single-channel current was about +30 mV. Under the conditions of the experiment, the external Mg^{2+} activity is calculated to be 17 mM and the internal Na^+ activity 120 mM (see Methods). Using these values and the Goldman–Hodgkin–Katz current equation, the permeability ratio between Mg^{2+} and Na^+ ($P_{Mg^{2+}}/P_{Na^+}$) is 24. This value is higher than the permeability ratio for ACh receptors from frog muscle where $P_{Mg^{2+}}/P_{Na^+}$ is between 0·2 and 0·3 (Adams *et al.* 1980).

Some of the observations presented here agree with those reported by Neuhaus & Cachelin (1990). Studying the effects of Mg^{2+} on PC12 ACh receptor single-channel currents, they also noted that the blocking by Mg^{2+} is asymmetrical, intracellular Mg^{2+} being more effective than extracellular Mg^{2+}. Although direct comparisons are difficult because Neuhaus and Cachelin used Cs^+ as the major cation in their solutions instead of Na^+, the concentration dependence and the degree of the block were similar to what was described here. However, there are some differences. Neuhaus and Cachelin reported little voltage dependence in the effects of Mg^{2+}, contrary to what was observed here. Also, they reported that external Mg^{2+} selectively modifies the inward conductance without affecting the outward conductance. Conversely, the effects of intracellular Mg^{2+} were on the outward currents and left the inward currents intact. This is also contrary to the results described in this paper. Neuhaus and Cachelin did not make any single-channel current measurements within 20 mV of the reversal potential and this may explain both the reported lack of voltage dependence in the block by Mg^{2+} and the sideness of the effect. Determining the *I–V* relationship around the reversal potential and determining the reversal potential are crucial in resolving the curvature of the single-channel *I–V* relationships since the curvature in these *I–V* curves is most apparent close to the reversal potential. The observed lack of effect of extracellular Mg^{2+} on outward currents which they report may be due to the fact that they measured slope conductances instead of chord conductances. Our results indicate that the slope of the *I–V* relationship for the outward currents reaches an asymptotic value positive to about +30 mV (see Fig. 4). Determining the *I–V* relationship at potentials positive to +30 mV, one could be

led to the conclusion that external Mg^{2+} has no effect on outward currents. Similarly with internal Mg^{2+}, the inward slope conductances appear to reach a limiting value (see Fig. 2). Therefore, we feel that there is no major difference between the data in their study and those in the present work.

Divalent cations are able to decrease the conductance of muscle ACh receptor channels (Adams *et al.* 1980; Magleby & Weinstock, 1980; Imoto *et al.* 1986, 1988; Dani & Eisenman, 1987; Decker & Dani, 1990). According to the model proposed by Dani & Eisenman (1987), muscle receptors are more effectively blocked by a given concentration of Mg^{2+} applied extracellularly than intracellularly, in contrast to PC12 cell ACh receptors which are more susceptible to block by intracellular Mg^{2+}. Like PC12 cell receptor channels, the block is consistent with open-channel block and permeation of Mg^{2+}. The effects of divalent cations on muscle ACh receptor channels are consistent with a one site, two barrier ion permeation model (Dani & Eisenman, 1987; Decker & Dani, 1990).

Although the structural basis for differences in the effects of Mg^{2+} between muscle-type and PC12 cell receptors has not yet been determined, studies of muscle and *Torpedo* nicotinic ACh receptors using site-directed mutagenesis have determined some of the amino acid residues that influence Mg^{2+} sensitivity and ion permeation through the channel (Imoto *et al.* 1986, 1988; Leonard *et al.* 1988). These residues are in or near the second membrane spanning region, M2, that has been proposed to form the lining of the channel pore (see Dani, 1989, for review). Of particular interest are three rings of residues that bracket the M2 region. For *Torpedo* receptors, Imoto *et al.* (1988) have shown that amino acid substitutions that increase the net negative charge on these rings can increase the sensitivity of the channel to Mg^{2+} and conversely, decreasing the net negative charge reduces the sensitivity. Therefore, it is possible that some of the differences between the effects of Mg^{2+} on muscle-type and PC12 ACh receptors can be explained by differences in the amount of charge on these crucial rings. At present, the subunit composition of the nicotinic receptors expressed by PC12 cells is not known. However, comparison of the subunits known to be expressed in PC12 cells to those of muscle in the M2 membrane-spanning regions and flanking sequences suggests that the residues in the charged rings cannot simply explain the features of Mg^{2+} block.

The data presented indicate that Mg^{2+} ions can block ion permeation through the neuronal nicotinic ACh receptor channels, and do so in a fashion qualitatively consistent with block following occupancy of a site in the permeation pathway. Our previous work has shown that channel block by internal Mg^{2+} can influence the shape of the whole-cell current–voltage relationship. However, it is clear that even in the absence of internal Mg^{2+} some rectification of whole-cell current remains (Yawo, 1989; Mathie *et al.* 1990; Neuhaus & Cachelin, 1990; Ifune & Steinbach, 1991).

This work was supported by grant R01 NS 22356 from the National Institutes of Health (J.H.S.) and training grant 2T32 HL07275-11 from the Department of Health and Human Services (C.K.I.). The authors thank C. Kopta, C. Lingle and J. Zempel for discussions and the critical reading of the manuscript.

REFERENCES

ADAMS, D. J., DWYER, T. M. & HILLE, B. (1980). The permeability of endplate channels to monovalent and divalent metal cations. *Journal of General Physiology* **75**, 493–510.

ALMERS, W. & MCCLESKY, E. W. (1984). Non-selective conductance in calcium channels of frog muscle: calcium selectivity in a single-file pore. *Journal of Physiology* **353**, 585–608.

ALMERS, W., MCCLESKEY, E. W. & PALADE, P. T. (1984). Non-selective cation conductance in frog muscle membrane blocked by micromolar external calcium ions. *Journal of Physiology* **353**, 565–583.

BALLIVET, M., NEF, P., COUTURIER, S., RUNGGER, D., BADER, C. R., BERTRAND, D. & COOPER, E. (1988). Electrophysiology of a chick neuronal nicotinic acetylcholine receptor expressed in *Xenopus* oocytes after cDNA injection. *Neuron* **1**, 847–852.

BUTLER, J. N. (1968). The thermodynamic activity of calcium ion in sodium chloride–calcium chloride electrolytes. *Biophysical Journal* **8**, 1426–1433.

COHEN, I. & VAN DER KLOOT, W. (1978). Effects of $[Ca^{2+}]$ and $[Mg^{2+}]$ on the decay of miniature endplate currents. *Nature* **271**, 77–79.

DANI, J. A. (1989). Site-directed mutagenesis and single-channel currents define the ionic channel of the nicotinic acetylcholine receptor. *Trends in Neurosciences* **12**, 125–128.

DANI, J. A. & EISENMAN, G. (1987). Monovalent and divalent cation permeation in acetylcholine receptor channels: ion transport related to structure. *Journal of General Physiology* **89**, 959–983.

DECKER, E. R. & DANI, J. A. (1990). Calcium permeability of the nicotinic acetylcholine receptor: the single-channel calcium influx is significant. *Journal of Neuroscience* **10**(10), 3413–3420.

DERKACH, V. A., SELYANKO, A. A. & SKOK, V. I. (1983). Acetylcholine-induced current fluctuations and fast excitatory post-synaptic currents in rabbit sympathetic neurones. *Journal of Physiology* **336**, 511–526.

FIEBER, L. A. & ADAMS, D. J. (1991). Acetylcholine-evoked currents in cultured neurones dissociated from rat parasympathetic cardiac ganglia. *Journal of Physiology* **434**, 215–237.

FUKISHIMA, Y. & HAGIWARA, S. (1985). Currents carried by monovalent cations through calcium channels in mouse neoplastic B lymphocytes. *Journal of Physiology* **358**, 255–284.

GIRAUDAT, J., DENNIS, M., HEIDMANN, T., CHANG, JUI-Y. & CHANGEUX, J. P. (1986). Structure of the high-affinity binding site for noncompetitive blockers of the acetylcholine receptor: Serine-262 of the δ subunit is labeled by [^{3}H]chlorpromazine. *Proceedings of the National Academy of Sciences of the USA* **83**, 2719–2723.

GOLDBERG, R. N. & NUTTALL, R. L. (1978). Evaluated activity and osmotic coefficients for aqueous solutions: the alkaline earth metal halides. *Journal of Physical and Chemical Reference Data* **7**, 263–310.

GRAHAME, D. C. (1947). The electrical double layer and the theory of electrocapillarity. *Chemistry Review* **41**, 441–501.

HATANAKA, H. (1981). Nerve growth factor-mediated stimulation of tyrosine hydroxylase activity in a clonal rat pheochromocytoma cell line. *Brain Research* **222**, 225–233.

HILLE, B., WOODHULL, A. M. & SHAPIRO, B. I. (1975). Negative surface charge near sodium channels of nerve: divalent ions, monovalent ions, and pH. *Philosophical Transactions of the Royal Society* B **270**, 301–318.

HIRANO, T., KIDOKORO, Y. & OHMORI, H. (1987). Acetylcholine dose–response relation and the effect of cesium ions in the rat adrenal chromaffin cell under voltage clamp. *Pflügers Archiv* **408**, 401–407.

HUCHO, F., OBERTHUR, W. & LOTTSPEICH, F. (1986). The ion channel of the nicotinic acetylcholine receptor is formed by the homologous helices MII of the receptor subunits. *FEBS Letters* **205**, 137–142.

IFUNE, C. K. & STEINBACH, J. H. (1990*a*). Regulation of sodium currents and acetylcholine responses in PC12 cells. *Brain Research* **506**, 243–248.

IFUNE, C. K. & STEINBACH, J. H. (1990*b*). Rectification of acetylcholine-elicited currents in PC12 pheochromocytoma cells. *Proceedings of the National Academy of Sciences of the USA* **87**, 4794–4798.

IFUNE, C. K. & STEINBACH, J. H. (1991). Inward rectification of nicotinic currents in PC12 cells: reduced internal divalent cation concentrations reveal a divergence between single channel and whole-cell currents. *Biophysical Journal* **59**, 445a.

IMOTO, K., BUSCH, C., SAKMANN, B., MISHINA, M., KONNO, T., NAKAI, J., BUJO, H., MORI, Y., FUKUDA, K. & NUMA, S. (1988). Rings of negatively charged amino acids determine the acetylcholine receptor channel conductance. *Nature* **355**, 645–648.

IMOTO, K., METHFESSEL, C., SAKMANN, B., MISHINA, M., MORI, Y., KONNO, T., FUKUDA, K., KURASAKI, M., BUJO, H., FUJITA, Y. & NUMA, S. (1986). Location of a δ-subunit region determining ion transport through the acetylcholine receptor channel. *Nature* **324**, 670–674.

LEONARD, R. J., LABARCA, C. G., CHARNET, P., DAVIDSON, N. & LESTER, H. A. (1988). Evidence that the M2 membrane-spanning region lines the ion channel pore of the nicotinic receptor. *Science* **242**, 1578–1581.

LEWIS, C. A. (1979). Ion-concentration dependence of the reversal potential and the single channel conductance of ion channels at the frog neuromuscular junction. *Journal of Physiology* **286**, 417–445.

MACONOCHIE, D. J. (1990). A study of the adrenal chromaffin nicotinic receptor using patch clamp and fast solution change techniques. Ph.D. dissertation. King's College, Strand, London.

MAGLEBY, K. L. & WEINSTOCK, M. M. (1980). Nickel and calcium ions modify the characteristics of the acetylcholine receptor–channel complex at the frog neuromuscular junction. *Journal of Physiology* **299**, 203–218.

MARTELL, A. E. & SMITH, R. M. (1974). *Critical Stability Constants*. Plenum Press, New York, London.

MATHIE, A., COLQUHOUN, D. & CULL-CANDY, S. G. (1990). Rectification of currents activated by nicotinic acetylcholine receptors in rat sympathetic ganglion neurones. *Journal of Physiology* **427**, 625–655.

MATHIE, A., CULL-CANDY, S. G. & COLQUHOUN, D. (1987). Single-channel and whole-cell currents evoked by acetylcholine in dissociated sympathetic neurons of the rat. *Proceedings of the Royal Society* **232**, 239–248.

MULLE, C. & CHANGEUX, J. P. (1990). A novel type of nicotinic receptor in the rat central nervous system characterized by patch-clamp techniques. *Journal of Neuroscience* **10**, 169–175.

MULLER, R. U. & FINKELSTEIN, A. (1974). The electrostatic basis of Mg^{2+} inhibition of transmitter release. *Proceedings of the National Academy of Sciences of the USA* **71**, 923–926.

NEUHAUS, R. & CACHELIN, A. B. (1990). Changes in the conductance of the neuronal nicotinic acetylcholine receptor channel induced by magnesium. *Proceedings of the Royal Society* B **241**, 78–84.

SHATKAY, A. (1968). Individual activity of calcium ions in pure solutions of $CaCl_2$ and in mixtures. *Biophysical Journal* **8**, 912–919.

WOODHULL, A. M. (1973). Ionic blockage of sodium channels in nerve. *Journal of General Physiology* **61**, 687–708.

YAWO, H. (1989). Rectification of synaptic and acetylcholine currents in the mouse submandibular ganglion cells. *Journal of Physiology* **417**, 307–322.

ZHANG, Z. W. & FELTZ, P. (1990). Nicotinic acetylcholine receptors in porcine hypophyseal intermediate lobe cells. *Journal of Physiology* **422**, 83–101.